ELSEVIER

Three-dimensional lipophilicity characterization of molecular pores and channel-like cavities

Gustavo A. Arteca and David R. Van Allen

Département de Chimie et Biochimie, Laurentian University, Sudbury, Ontario, Canada

Molecular lipophilicity is a useful property for assessing molecular similarity or complementarity within the context of computer-aided drug design. As well, local contributions to solvent affinity help us to understand both dynamics and conformational stability in biomolecules. In this work, we discuss an approach to characterize the local contributions to hydrophobicity by using one- and two-dimensional representations of molecular channel-like cavities. The method monitors how a phenomenological lipophilicity potential (based on fragmental atom contributions) changes over a continuum of "molecular tubes" used for modeling channels and pores. Our results convey a relatively detailed picture of the spatial distribution of water affinity. The procedure can then be used as a complement to the hydrophobicity scales based on averaging contributions from single amino acids. In addition, we can study how the water affinity changes for inner and outer regions of the pores. As an application, we compute the 3D distribution of lipophilicity in the "pore conformation" of gramicidin A. The qualitative trends indicated by our results are broadly consistent with computer simulations of the gramicidin channel in the presence of hydrated ions. The behavior revealed by the simulations can then be incorporated to produce an improved, simple 2D model for water–channel interactions. © *1996 by Elsevier Science Inc.*

INTRODUCTION

The biochemical activity associated with a molecule can be correlated with several properties, including nuclear geometry, bond topology, molecular electrostatics, and solvent affinity. The latter is the most difficult, since there is no simple approach for its computation. Yet, hydropathicity (a term encompassing hydrophobicity to hydrophilicity)[1] is an important factor that must be taken into account when designing receptor ligands or understanding solvation dynamics in biomolecules. Here, we are interested in optimizing an approach for the display and analysis of local hydrophobicity in membrane proteins associated with ion transport. (As it is customary, we use the term *lipophilicity* as a synonym of *hydrophobicity*.)

The hydropathicity of an entire molecule is usually quantified in terms of the logarithm of the macroscopic partition coefficient between a pair of immiscible solvents,[2] log P. This property follows approximate additivity relations over functional groups present in the molecule. Thus, it is possible to assign lipophilicity contributions to various molecular fragments, from conveniently defined "atom types"[3,4] to entire amino acid residues.[5,6] Consequently, the hydrophobicity of a group of atoms inside a molecule can be estimated. Various scales of hydrophobicity for biomolecules are based on these principles,[7–11] and are commonly implemented in standard programs used in molecular biology.[12] These techniques, however, do not differentiate between regions in space about a group of atoms. Yet, the spatial dependence of lipophilicity, rather than its dependence on composition, is probably the most relevant aspect for molecular recognition. For this reason, several approaches to estimate the three-dimensional (3D) distribution of solvent affinity have been developed. These include the use of molecular electrostatics[13] and heuristic "lipophilicity potentials" constructed from fragmental additivity of log P.[14–18] Lipophilicity potentials are usually displayed on solvent-accessible molecular surfaces.[15–19] In this work, we implement an alternative representation, adapted to the analysis of channel-like cavities. Using this approach, we study 3D lipophilicity profiles and compare them with composition-dependent hydropathicity scales. The present method is proposed as an improved alternative to display and characterize water–channel interactions, at a minimal computational cost.

Address reprint requests to: Dr. Arteca, Département de Chimie et Biochimie, Laurentian University, Ramsey Lake Road, Sudbury, Ontario, Canada P3E 2C6.

Received 30 May 1996; revised 23 October 1996; accepted 24 October 1996.

655 Avenue of the Americas, New York, NY 10010

0263-7855/96/$15.00
SSDI 0263-7855(96)00076-8

GENERAL PROPERTIES OF GRAMICIDIN A CHANNELS

We are interested in characterizing lipophilicity by means of simple 1D and 2D models of channel-like cavities. It must be noted that we shall deal with cases where these cavities are nonuniform. (For a general overview of the typical structures found in membrane channels, as well as their biological functions, see Ref. 20.) In these situations, the geometric representations required will not be regular. That is, the 1D model used will not be perfectly linear, nor will the 2D model be perfectly cylindrical.

As an illustrative example of a biomolecular system with these features, we consider here a well-characterized form of the transport channel of gramicidin A. (For a general introduction see Refs. 21–23.) Gramicidin A, a polypeptide extracted from *Bacillus brevis*, includes mostly hydrophobic residues and can insert itself into phospholipid membranes.[21] In that position, it is known to selectively transport monovalent cations.[24] The channel is impermeable to other cations and all anions. Its biological role as an antibiotic might be related to its capacity to transport K^+ ions into the mitochondria.[21,22] The channel-like cavity is spanned by two identical helical 15-residue chains. Each chain contains valine (V), glycine (G), alanine (A), leucine (L), and tryptophan (W), with the composition: HCO-[VGALAVVVWLWLWLW]-NH-$(CH_2)_2$OH. The C-terminal residue (residue 1 or "tail") is L-valine; the following residues alternate L and D chiralities. Owing to this unusual alternancy, gramicidin A dimers can adopt various conformations not commonly accessible to other peptides. In our particular case, we deal with the so-called antiparallel double-stranded (APDS) β helix, where one chain monomer winds around the other. In this conformation, also known as a "pore,"[21] the two monomers are doubly stranded in a head-to-tail fashion. That is, the N terminal of one chain neighbors to the C terminal of the other chain. This structure should not be confused with the more common "gramicidin channel" (or HH, "head-to-head" conformer), which is a channel spanned by two contiguous helices. In the HH arrangement, the N terminal of one monomer is electrostatically attached to the N terminal of the other in the middle of the cellular membrane.[21] This latter conformer is believed to be the most common form of the gramicidin channel in actual membranes.

Many simulation studies have addressed the issue of ion selectivity and water dynamics in gramicidin A.[25–37] Representative approaches have mostly dealt with the HH dimer channel, using Monte Carlo simulations,[26,27] dipolar models of the channel interior,[29,31,37] polyalanine models,[33] as well as molecular dynamics including water molecules[32,34] and a model membrane.[35,36] Some work has also been performed on structural[38] and dynamic[30] properties of the APDS gramicidin pore. Computations on both conformers indicate a high potential energy barrier for the desolvation of anions. This accounts for the ionic selectivity, since desolvation is a required step for migration across the channel. A lower conductivity is expected for the gramicidin pore because its potential energy barriers for ion transport are larger than those for the HH channel.[30] From the viewpoint of lipophilicity, the APDS gramicidin conformer is a more challenging problem, since its intertwined chains should give rise to a more pronounced spatial dependence of water affinity along the pore. In this work, we restrict our analysis to the latter conformer.

Computer simulations of water dynamics inside the gramicidin pore indicate preferential binding toward the mouths of the cavity, at ca. 13 Å of the pore's midpoint. The results are also dependent on the actual position along the channel, since the pore dimensions are quite irregular, in particular for the ion-free cavity.[38] Such irregularities, which distort a channel from cylindrical symmetry, appear to play a key role in regard to water permeability and ion desolvation.[38–40] (The ion-bound channel has a more regular structure, resulting from the deformation of the gramicin backbone induced by the internally bound cation.)

In summary, detailed dynamics simulations provide a first-principles description of water affinity, which can then be compared with simpler phenomenological models. As discussed above, these simpler approaches can either provide a measure of hydrophobicity based on the primary sequence of the polypeptide or on the spatial dependence of the lipophilicity potential. In this work, we present results from the latter approach. The lipophilicity potential is computed on a realistic "molecular tube" winding through the gramicidin A pore.

For the sake of comparison, we can briefly analyze the results provided by other hydropathicity scales. Figure 1 presents three standard measures, based on (1) the local hydrophobicity of Hopp and Woods[7] (using a 9-residue group length averaging), (2) the hydropathicity index of Kyte and Doolittle,[1] and (3) the hydrophobic moment of Eisenberg et al.[8–10] (with an 11-residue averaging window,

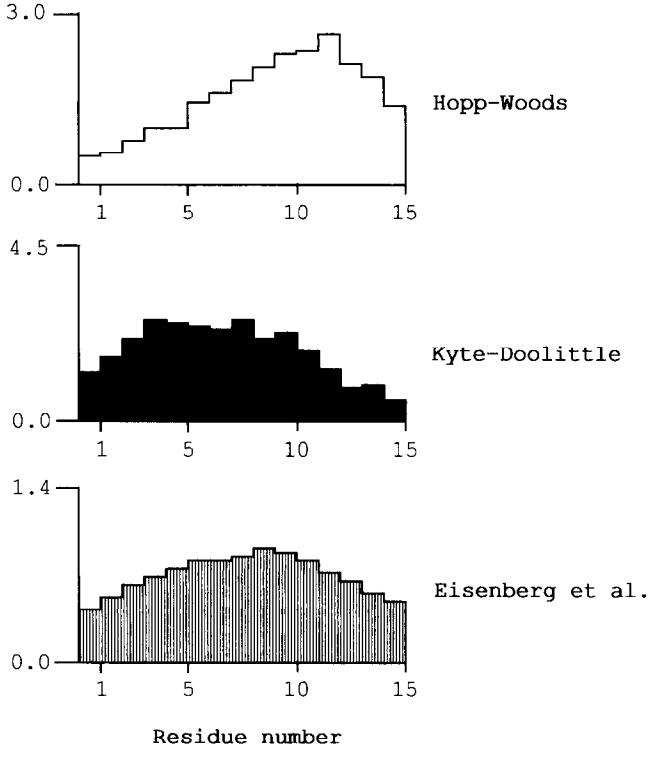

Figure 1. Sequence-dependent hydropathicity scales for a single chain of gramicidin A. (See text for the references to the methods.)

and a fixed angle of 100° for the orientation of side chains to a regular helical axis). The results in Figure 1 are only slightly affected by the use of smaller windows for averaging. Even though all scales indicate an increasing hydrophobicity toward the middle of a gramicidin chain, they do not agree on the location of the lipophilicity maximum. Later, we compare these scales with those from a geometry-dependent measure of lipophilicity.

DETERMINATION OF CHANNEL AXES AND MOLECULAR TUBES

Under the appropriate experimental conditions, the antiparallel double helix is believed to be a possible conformer of the membrane-bound gramicidin A.[20,40] The X-ray crystal structure of the ion-free APDS gramicidin A pore is found in the Brookhaven Protein Data Bank (PDB)[41] under the code 1GMA.[42,43] These coordinates already include hydrogen atom positions and the correct chirality. This ion-free pore is a fairly long (30 Å), narrow (~4-Å diameter), and irregular structure. The effect of these irregularities on pore dimensions has been discussed in detail by Smart et al.[38] Therefore, a proper modeling should take into account the noncylindrical nature of the pore, and derive accordingly a "molecular surface" that is deformed along the cavity. (The occurrence of irregularities in membrane pores is a general feature found in many other examples.[20]) As commented on above, we consider here the case of APDS gramicidin A, instead of the HH conformer, since this latter should exhibit a stronger spatial dependence of lipophilicity. Note that in APDS we have two polypeptidic chains with the same composition, but intertwined in head-to-tail fashion. For this reason, methods that characterize molecular hydropathicity from the primary sequence of a single chain will not perform well when applied to a structure such as the APDS conformer.

There are several alternative approaches to display and analyze polypeptide surfaces and cavities.[44–50] However, using van der Waals, solvent-accessible, or spherical harmonics surfaces may not be appropriate for an analysis of internal and external surfaces about ion channels.[37] First, it is difficult to display only the section of the surface in which one is interested, e.g., the inner pore. Second, standard molecular surfaces are defined as an envelope of spheres centered about the nuclei,[47] and therefore they provide a better model for the regions near the channel walls. However, molecular dynamics simulations indicate that solvent molecules and ions travel near the center of the pore and do not approach its walls.[30,37–39] Thus, in the present work we are interested in monitoring "cylindrical surfaces" defined about an axis tracing the pore, rather than the van der Waals surfaces defined by the channel atoms.

For the above reasons, we resort to an alternative approach in order to construct the "molecular tube." The method involves two steps: (1) an axis winding about the molecular channel is determined; (2) a distribution of radial points (the "molecular tube") is generated at a desired distance from the channel axis. The calculations are performed with the program *Mol_Tube*.CPP, written in standard C++, and run on a personal computer.[51]

We have tested two techniques to compute a one-dimensional molecular axis for the channels. One of the algorithms can be considered a simplification of the method used in Ref. 38 to compute the gramicidin A axis. The second approach is based on iterated cubic splines built from the backbone α-carbon atoms.[52,53] The first method, which we describe briefly below, appears to be the most convenient for channel-like cavities.

Method

Let $\{\mathbf{r}_i, i = 1,2, \ldots, N\}$ be the nuclear coordinates of a biomolecule with N atoms (as found in a PDB entry). (In our present example, we find N = 544 for the two main chains of gramicidin A, i.e., for residues 1–15.) In our algorithm, the axis is determined as follows:

1. The user provides two points $\mathbf{p}_I$ and $\mathbf{p}_F$, roughly located at the mouths of the channel. Thus, the vector $\mathbf{v}_0 = \mathbf{p}_F - \mathbf{p}_I$ points approximately in the direction of the channel. (The choice of initial points is easily made by using molecular modeling packages. In our case, we used the program *HyperChem*[54] to display the PDB file and determine the input data for our program.)
2. The axis is built as a *constrained walk* inside the channel. The steps of the walk correspond to points situated on specially chosen planes across the channel. To start, the user specifies a distance, "a" (in angstroms), between these planes. (Alternatively, one can specify the rough number points desired for the axis.) This distance, a controls the precision of the calculation. The axis path is parametrized in terms of "*d*," the *fractional distance* with respect to the total length of the walk. Accordingly, we indicate the axis points by the set: $\{\mathbf{p}_j = \mathbf{r}_A(d_j), j = 1, 2, 3, \ldots; d_j \epsilon I = [0,1]\}$. In addition, the user can specify a distance cutoff, S, in order to define a region in which to seek the atoms that are relevant to determining a particular axis point.
3. The determination of the first point of the axis, $\mathbf{p}_1 = \mathbf{r}_A(d_1)$, is as follows. Starting from $\mathbf{p}_I$ we reach a new point $\mathbf{p}_1'$ by taking a step of length a along the given vector ($\mathbf{v}_0$) pointing to the channel, $\mathbf{p}_1' = \mathbf{p}_I + a\,\mathbf{v}_0/\|\mathbf{v}_0\|$. Then, a plane perpendicular to $\mathbf{v}_0$ at the intermediate point $\mathbf{p}_1'$ is determined. One of such general planes, associated with the axis point $\mathbf{p}(d_j)$, will be indicated as "plane(d_j)." The corresponding "direction vector," leading to this plane from the previous axis point $\mathbf{p}(d_{j-1})$, will be denoted by $\mathbf{v}(d_{j-1})$. With this notation, the initial vector $\mathbf{v}_0$ becomes $\mathbf{v}(d_0)$.
4. A search is then performed within plane(d_1) in order to find a new point, $\mathbf{r}_A(d_1)$, that minimizes the mean distances to the nuclei found within the *S*-distance cutoff to the point $\mathbf{p}_1'$. That is, we determine a point on plane(d_1) that is most centrally located on the channel cross-section. The point thus found becomes $\mathbf{r}_A(d_1)$, the first for the axis.
5. The new direction vector $\mathbf{v}(d_1) = \mathbf{r}_A(d_1) - \mathbf{p}_I$ is used to compute the next axis point. The procedure continues as above. An intermediate point, $\mathbf{p}_2' = \mathbf{r}_A(d_1) + a\,\mathbf{v}(d_1)/\|\mathbf{v}(d_1)\|$, is reached and the plane(d_2)$\perp\mathbf{v}(d_1)$ is determined. Then, a constrained search within the plane is performed and a new point is obtained. This becomes the pivot for the next axis point, and so forth.

6. During the calculation, an approximate channel axis is estimated to monitor whether one has reached the end of the pore. The coordinates of the channel atoms are projected onto the approximate axis, their values are compared to the last axis point computed. If some projected atomic coordinates appear further along the approximate axis, the point is still inside the pore.

The ensemble of axis points $\{\mathbf{r}_A(d_j), j = 1, 2, 3, \ldots\}$ is denoted by **A.** In summary, these points are determined as

$$\mathbf{A} = \left\{ \mathbf{r}_A(d_j): \mathbf{r}_A \in \text{plane}(d_j), \text{ with: } \min \sum_i \| \mathbf{r}_A - \mathbf{r}_i \|^2, \text{ if } \| \mathbf{r}_A - \mathbf{r}_i \| < S \right\} \quad (1)$$

where: $\text{plane}(d_j) \perp \mathbf{v}(d_{j-1}) = \mathbf{r}_A(d_{j-1}) - \mathbf{r}_A(d_{j-2})$. In the present approach, we have used a distance constraint between the axis points and the nuclear positions. Other alternatives can also be used. For instance, one can take into account the distances to the corresponding van der Waals (atomic) spheres or introduce an appropriate Boltzmann statistical weight factor for nuclei–axis distances.[38]

Once the axis **A** is known, a tube winding through the pore (or enclosing it from the outside) can easily be determined. A possible representation for a "molecular tube of radius *R*" is a series of points within each plane(d_j), at a distance R from the axis **A.** These points can be parameterized by the fractional distance d_j and an angle ϕ. In the simplest approach, we generate a regular distribution of n points within plane(d_j), by using multiples of the angle $\phi = 2\pi/n$. These parameters are schematically indicated in Figure 2. Figure 2 also shows a generic axis point at a fractional distance d; the points indicated as "0" and "1" are located at the mouths of the channel. Finally, using the notation in Eq. (1), we can indicate the resulting 2D tube by the ensemble $\mathbf{T}_R$:

$$\mathbf{T}_R = \{\mathbf{r}_T(d_j, \phi): \mathbf{r}_T \in \text{plane}(d_j), \text{ with: } \|\mathbf{r}_T(d_j, \phi) - \mathbf{r}_A(d_j)\| = R\} \quad (2)$$

Other options are also possible to construct the tubes, e.g., by using a random distribution of points about the pore axis.

The construction of the axial points $\{\mathbf{r}_A\}$ is the determining step for the calculation. The algorithm scales with the number of atoms as N^2. The evaluation of a high-resolution axis for gramicidin A (e.g., a = 0.1Å) takes approximately 12 min CPU on a PC-486/33 platform. From this high-resolution axis, the user can choose the actual resolution desired for the final tube, by establishing how many points along the axis will be retained, as well as the value of the angle ϕ for scanning. If desired, the resulting tube points can be checked for atomic contacts with van der Waals radii, although we have not used this option here. From the high-resolution axis, the computation of molecular tube vectors $\{\mathbf{r}_T\}$ for an R = 1 Å tube, with $\phi = 30°$, takes ca. 2 sec CPU on the same PC. Results are similar for all other tubes tested in this work.

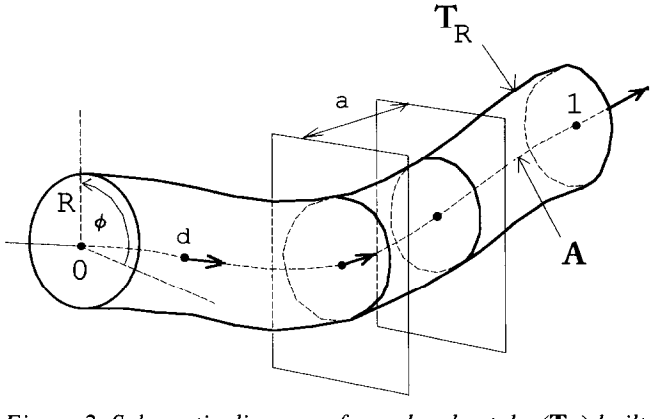

*Figure 2. Schematic diagram of a molecular tube ($\mathbf{T}_R$) built around a molecular axis (**A**). (In order to determine the tube points, the user must supply the parameters R, ϕ, a, as well as two initial points located at the mouths of the pore.)*

Figure 3 shows two views of the gramicidin A axis resulting from a high-resolution (a = 0.1 Å) computation, followed by a selection of points separated by ca. 0.5 Å. (This smaller accuracy, requiring the computation of lipophilicity over a much smaller set of points, is sufficient for our present analysis.) For reference, Figure 3 (displayed with RasMol[55]) highlights the backbones of the main chains of each gramicidin A monomer. As Figure 3 suggests, the 0.5-Å resolution path describes correctly the irregularities along the cavity. Once the path is determined, one can assess its shape features quantitatively and compare it with the axis associated with a regular β helix. Techniques for the molecular shape analysis of 1D molecular backbones are discussed in Refs. 56 and 57.

Figure 4 shows two views of the molecular tube $\mathbf{T}_R$, with R = 1 Å and $\phi = 30°$. This 2D model provides a reasonable description of the environment inside the gramicidin A pore. The orientation of the tube points with respect to the amino acid residues is clarified in Figure 5. Figure 5 gives the (d, ϕ) values of the tube point closest to each of the α carbons. The diagram illustrates clearly the antiparallel double-stranded helical nature of the dimer. The local contribution of one amino acid residue to the 2D lipophilicity maps can be interpreted with this plot.

We have used this algorithm to produce a number of molecular tubes with desired dimensions. Once a distribution of tube points is obtained, it is possible to monitor any physical property in regions that have the same symmetry as the channel. In the next section, we show the results for the lipophilicity potential along the pore axis and for different molecular tubes.

LIPOPHILICITY POTENTIAL MAPS FOR GRAMICIDIN AXIS AND MOLECULAR TUBES

A phenomenological lipophilicity function (or "potential") can be constructed for qualitatively mapping solvent affinity around a molecule. The functions designed to date, although built in analogy to the electrostatic potential, are heuristic and not based on rigorous physical principles.[14–18,58] These potentials assign a value to the lipophilicity at a point **r** in space, using the contribution to the partition coefficient (f_i) of an atomic fragment located at a point $\mathbf{r}_i$ Their general form can be represented by

$$L(\mathbf{r}) = \sum_{i=1}^{N} f_i \, g(\|\mathbf{r} - \mathbf{r}_i\|) \quad (3)$$

with some smooth function $g(\|\mathbf{r} - \mathbf{r}_i\|)$. This function is introduced to mimic how the interaction of one atom with

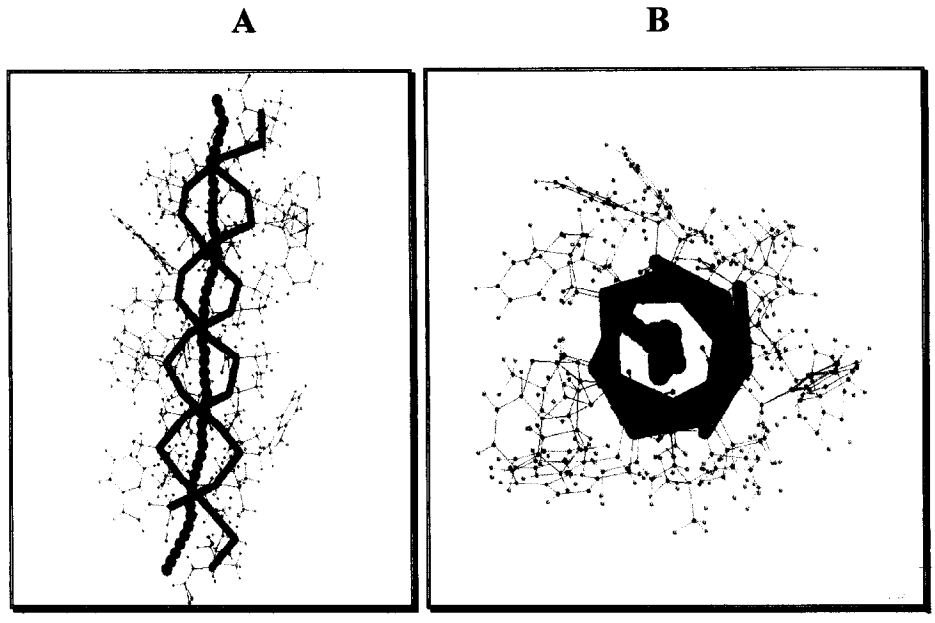

Figure 3. Two views of an axis winding along the gramicidin A pore. (The points are approximately separated by 0.5 Å, and are selected from a higher resolution computation of an axis with a = 0.1 Å.)

the solvent is somehow "screened" by the presence of the other. A number of choices have been proposed in the literature, based on rather loose criteria.[14–18] Ultimately, it is believed that, qualitatively, the spatial distribution of the lipophilicity potential L(**r**) should not be strongly dependent on the analytic form of the function $g(\|\mathbf{r} - \mathbf{r}_i\|)$.[17,18] For this reason, and in order to simplify our discussion, we have computed the lipophilicity potential using a single representation for the screening function.

In the present case, we resort to a simple Coulomb-type screening,[14,16] where $g(\|\mathbf{r} - \mathbf{r}_i\|) = 1/(1 + \|\mathbf{r} - \mathbf{r}_i\|)$. To use this expression, distances must be in angstrom: but the final L(**r**) value is taken as dimensionless. For the atomic fragmental contributions $\{f_i\}$ in Eq. (3), we use the results of Viswanadhan et al.,[4] who have assigned the values of 120 different "atom types." These atom types are determined automatically from the primary sequence in a PDB file by using an in-house program.[59]

We have computed the function L(**r**) for 1D and 2D models of gramicidin A. In this case, the position vectors {**r**} correspond to axis and molecular tube points, respectively. Note that we monitor regions of the pore defined by a molecular tube that does not take into account the atomic radii. However, the atomic sizes are indeed taken into account when computing the lipophilicity potential. An illustration of the results obtained is found in Figures 6 and 7.

Figure 6 shows the lipophilicity profile along the 1D gramicidin A axis. The L(**r**) values obtained are all positive, indicating that the interior of the pore is mostly hydrophobic. However, the diagram indicates clearly the presence of two less hydrophobic regions near the entrance and exit of the pore. Note that the most lipophilic region of the pore is not found in its middle, but rather at a fractional distance d $\approx$ 0.65. According to Figure 5, this region is not far from the tryptophan residue 11 in chain A, and the valine residue 6 in chain B. It is interesting to compare this result with the 1D

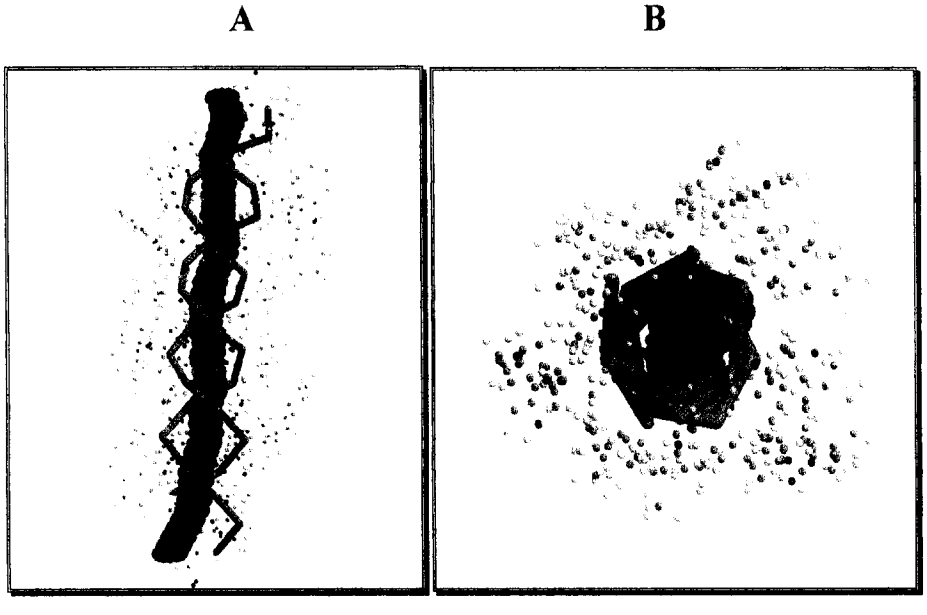

Figure 4. Two views of a molecular tube winding along the gramicidin A pore (radius = 1 Å). (The points are determined from the axis shown in Figure 3, using a $\phi = 30°$ angular scanning.)

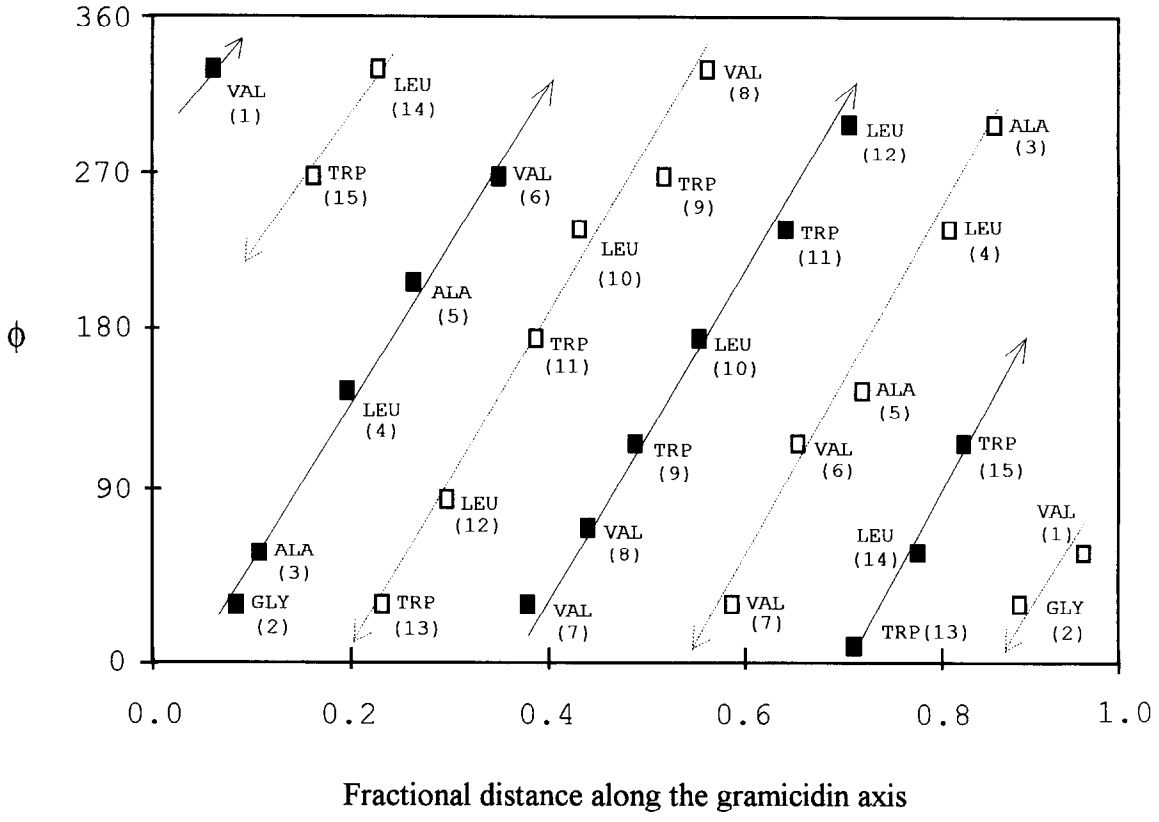

Figure 5. Approximate location of amino acid residues with respect to the distribution of points on a molecular tube for gramicidin A.

hydropathicity scales derived from the primary sequence (cf. Figure 1). According to the Hopp–Woods scale,[7] the most lipophilic position should be found about residue 12, whereas the Kyte–Doolittle scale[1] favors residue 6. By contrast, the scale of Eisenberg et al.,[8–10] gives a similar lipophilicity for residues 6 through 11. Our results seem to interpolate rather consistently between these discrepancies: the most hydrophobic region we find along the gramicidin axis is closer to residues 8–12 of chain A and residues 5–10 of chain B. Note that, despite the fact that APDS gramicidin is made of two identical chains, the profile in Figure 6 is not symmetrical about d = 0.5. This is because the interior of the channel is irregular in this conformation, and it clearly illustrates the importance of taking into account the actual spatial dependence of hydrophobicity.

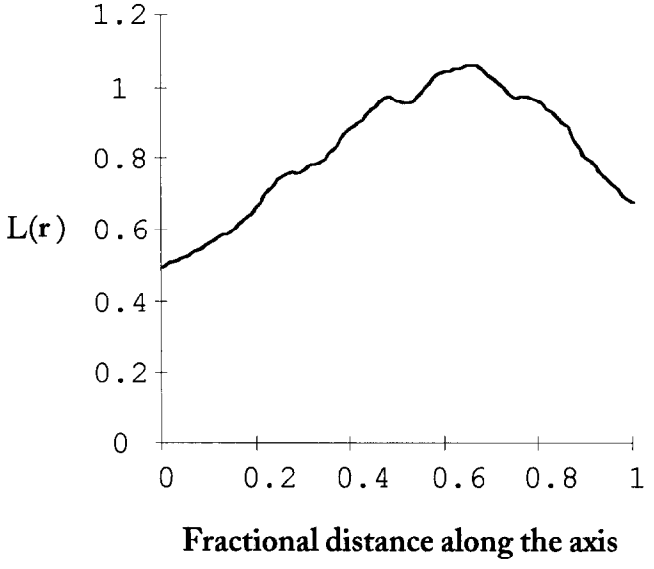

Figure 6. Lipophilicity potential profile associated with the 1D model of the gramicidin A pore. (The calculation uses the axis displayed in Figure 3.)

Figure 7 expands the description of gramicidin lipophilicity by contrasting inner and outer molecular tubes (top and bottom, respectively). The top of Figure 7 shows the 2D contours of lipophilicity potential corresponding to the tube displayed in Figure 4. This latter tube should be the most relevant to interpret water–channel interactions, since computer simulations predict that water molecules inside the APDS gramicidin channel a span single-file region, ca. 0.9 Å off-axis.[30] Similar qualitative behavior is also observed in the HH conformer.[26,27,29,32,33]

The lipophilicity contour map for the R = 1 Å tube is comparable to the profile in Figure 6. We find a "band" of larger hydrophobicity centered about d ≈ 0.65. For the molecular tube, this region is also affected by residues 8 and 14 in chain B, found at d ≈ 0.45 and d ≈ 0.80, respectively (cf. Figure 5). Nevertheless, the L(**r**) contours for the interior tube show, in general, little angular dependence for a given d value. This result suggests that water molecules penetrating the channel could vibrate symmetrically about positions perpendicular to the pore axis. This feature seems to agree

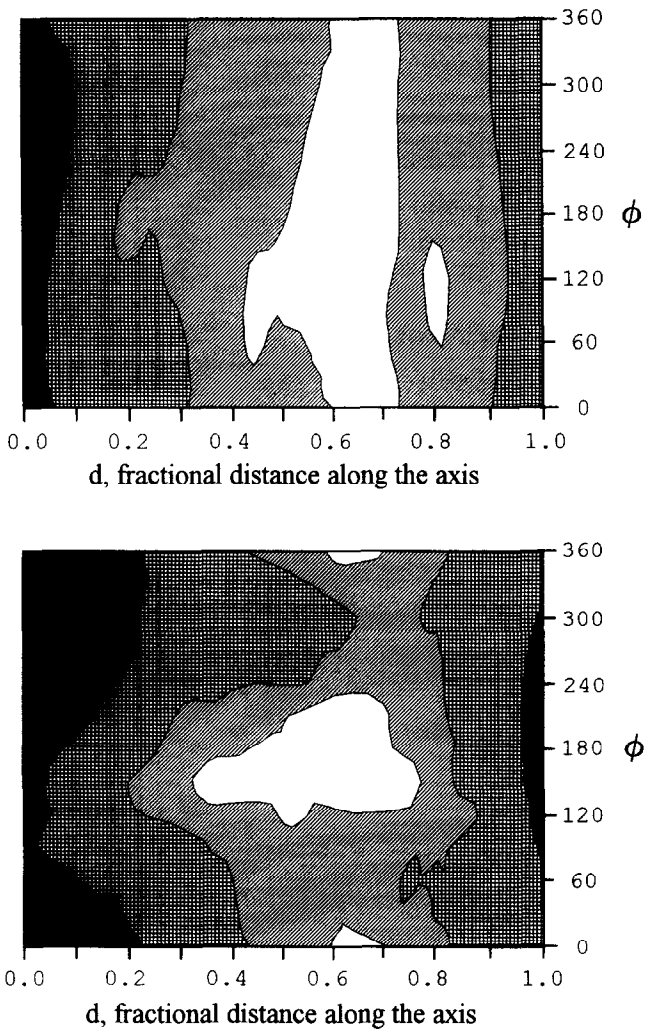

Figure 7. Two-dimensional lipophilicity maps for molecular tubes centered about the gramicidin A axis. (The top diagram corresponds to a radius of 1 Å from the axis and it is located inside the pore. The second diagram corresponds to a tube of 7-Å radius and it maps the outside of gramicidin A. Note the striking differences between the interior and the exterior of the channel. For the chemical groups associated with the various regions of the diagram, see Figure 5.)

with the results from computer simulations, indicating that water dipoles inside the pore are oriented, on average, in the same direction along the axis.[26,27,30]

The bottom diagram in Figure 7 allows us to see different features in APDS gramicidin when monitoring its exterior. Here, we find an extended hydrophobic region at $0.4 < d < 0.8$ and $\phi \sim 180°$. This region corresponds to residues 9–11 in both chains, and its hydropathicity agrees better with the Hopp–Woods scale. Moreover, solvent affinity appears to have a larger angular dependence at the exterior. These results illustrate again the importance of including the correct geometric information, in addition to the fragmental contribution to lipophilicity.

FURTHER COMMENTS AND CONCLUSIONS

In this work, we have implemented an algorithm to build 1D and 2D models of channel-like cavities and used it to monitor hydrophobicity in regions of interest. Note that, contrary to an analysis of lipophilicity on a van der Waals surface, the molecular tubes mimic correctly the shape features of the actual space explored by ions and water molecules during migration. As commented on above, ion and water molecules appear to follow mostly "single-curve" trajectories inside gramicidin.[30] Therefore, it is important to monitor hydrophobicity in tubelike spaces about the channel axes, rather than on other molecular surfaces. The 1D and 2D representations illustrated in this work incorporate any important irregularities found in actual molecular pores or channels. Such irregularities in pore size can play a central role in the dynamics of ion translocation.[38]

Our method highlights the importance of including geometric information when describing hydrophobicity in irregular biomolecular structures. Our results show that the use of a 3D approach complements the standard hydropathicity scales for peptides. In addition, as shown in the previous section, the analysis of lipophilicity along the proper channel axis may help to clarify some of mutual inconsistencies among such scales.

It should be clear that the present results provide only an approximate description of solvent affinity, because the lipophilicity potential is only a qualitative tool. Moreover, we have considered only a rigid conformation and neglected the vibrational coupling between water (or solvated ions) with the channel. Similarly, the role of an embedding membrane has not been taken into account. Nevertheless, some of these effects can be incorporated into our model. For instance, it could be possible to use the results of molecular dynamics (or Monte Carlo) simulations to recalibrate the fragmental contributions $\{f_i\}$ to lipophilicity. Such a recalibration

could possibly allow one to incorporate some of the actual effects found in realistic solvent–peptide interactions. Proceeding this way, it may be possible to design a more effective, mean lipophilicity function L(**r**) for the analysis of membrane-bound proteins. We believe that the approach in this work can be extended in this fashion, and then used to obtain reliable information on biomolecular cavities at a much lower computational cost.

REFERENCES

1 Kyte, J. and Doolittle, R.F. *J. Mol. Biol.* 1982, **157,** 105
2 Dunn, W.J., III, Block, J.H., and Pearlman, R.S., Eds. *Partition Coefficient Determination and Estimation.* Pergamon Press, New York, 1986
3 Ghose, A.K. and Crippen, G.M., *J. Comput. Chem.* 1986, **7,** 350
4 Viswanadhan, V.N., Ghose, A.K., Revankar, G.R., and Robins, R.K. *J. Chem. Inf. Comput. Sci.* 1989, **29,** 163
5 Levitt, M. *J. Mol. Biol.* 1974, **104,** 59
6 Eisenberg, D., Weiss, R.M., Terwilliger, T.C., and Wilcox, W. *Faraday Symp. Chem. Soc.* 1984, **81,** 140
7 Hopp, T.P. and Woods, K.R. *Proc. Natl. Acad. Sci. U.S.A.* 1981, **78,** 3824
8 Eisenberg, D., Weiss, R.M., Terwilliger, T.C. *Nature (London)* 1982, **299,** 371
9 Eisenberg, D., Weiss, R.M., and Terwilliger, T.C. *Proc. Natl. Acad. Sci. U.S.A.* 1984, **81,** 140
10 Eisenberg, D. and McLachlan, A.D. *Nature (London)* 1986, **319,** 199
11 Fraga, S., Parker, J.M.R., and Pocock, J.M. Lecture Notes in Chemistry, Vol. 66: *Computer Simulation of Protein Structures and Interactions.* Springer-Verlag, Berlin, 1995
12 DNA Star. *Protean (Lasergene for Windows).* DNA Star, Inc., Madison, Wisconsin, 1995
13 Kellog, G.E. and Abraham, D.J. *J. Mol. Graphics* 1992, **10,** 212
14 Audry, E., Dubost, J.-P., Colleter, J.-C., and Dallet, Ph. *Eur. J. Med. Chem.-Chim. Thér.* 1986, **21,** 71
15 Furet, P., Sele, A., and Cohen, N.C. *J. Mol. Graphics* 1988, **6,** 182
16 Croizet, F., Langlois, M.H., Dubost, J.P., Braquet, P., Audry, E., Dallet, Ph., and Colleter, J.C. *J. Mol. Graphics* 1990, **8,** 153
17 Heiden, W., Moeckel, G., and Brickmann, J. *J. Comput.-Aided Mol. Design* 1993, **7,** 503
18 Bone, R.G.A. and Villar, H.O. *J. Mol. Graphics* 1995, **13,** 201
19 Rozas, I., Du, Q., and Arteca, G.A. *J. Mol. Graphics* 1995, **13,** 98
20 Montal, M. *Curr. Opin. Struct. Biol.* 1996, **6,** 499
21 Wallace, B.A. *Annu. Rev. Biophys. Chem.* 1990, **19,** 127
22 Busath, D.D. *Annu. Rev. Physiol.* 1993, **55,** 473
23 Marshall, G.R., Beusen, D.D., and Nikiforovich, G.V. In: *Peptides: Synthesis, Structures, and Applications* (Gutte, B., Ed.). Academic Press, San Diego, California, 1995
24 Eisenman, G. and Horn, R. *J. Membr. Biol.* 1983, **76,** 197
25 Roux, B. and Karplus, M. *Biophys. J.* 1988, **53,** 297
26 Kim, K.S. and Clementi, E. *J. Am. Chem. Soc.* 1985, **107,** 5504
27 Kim, K.S., Vercauteren, D.P., Welti, M., Chin, S., and Clementi, E. *Biophys. J.* 1985, **47,** 327
28 Pullman, A. *Q. Rev. Biophys.* 1987, **20,** 173
29 Skerra, A. and Brickmann, J. *Biophys. J.* 1987, **51,** 969
30 Sung, S.-S. and Jordan, P.C. *Biophys. J.* 1988, **54,** 519
31 Åqvist, J. and Warshel, A. *Biophys. J.* 1989, **56,** 171
32 Chiu, S.-W., Subramaniam, S., Jakobsson, E., and McCammon, J.A. *Biophys. J.* 1989, **56,** 253
33 Roux, B. and Karplus, M. *Biophys. J.* 1991, **59,** 961
34 Chiu, S.-W., Jakobsson, E., Subramaniam, S., and McCammon, J.A., *Biophys. J.* 1991, **60,** 273
35 Roux, B. and Karplus, M. *J. Am. Chem. Soc.* 1993, **115,** 3250
36 Roux, B., Prod'hom, B., and Karplus, M. *Biophys. J.* 1995, **68,** 876
37 Dorman, V., Partenskii, M.B., and Jordan, P.C. *Biophys. J.* 1996, **70,** 121
38 Smart, O.S., Goodfellow, J.M., and Wallace, B.A. *Biophys. J.* 1993, **65,** 2455
39 Sansom, M.S.P., Kerr, I.D., Breed, J., and Sankararamakrishnan, R. *Biophys. J.* 1996, **70,** 693
40 Wolfe, S.L. *Molecular and Cellular Biology.* Wadsworth, Belmont, California, 1993
41 Bernstein, F.C., Koetzle, T.F., Williams, G.J.B., Meyer, E.F.J., Brice, M.D., Rodgers, J.R., Kennard, O., Shimanouchi, T., and Tasumi, M. *J. Mol. Biol.* 1977, **112,** 535 [Brookhaven PDB's WWW Address: http://pdb.pdb.bnl.gov]
42 Durkin, J.T., Andersen, O.S., Heitz, F., Trudelle, Y., and Koeppe, R.E., II. *Biophys. J.* 1987, **51,** 451
43 Langs, D.A. *Science* 1988, **241,** 188
44 Connolly, M.L. *Science* 1983, **221,** 709
45 Ho, C.M.W. and Marshall, G.R. *J. Comput.-Aided Mol. Design* 1990, **4,** 337
46 Levitt, D.G. and Banaszak, L.J. *J. Mol. Graphics* 1992, **10,** 229
47 Teschner, M., Henn, C., Vollhardt, H., Reiling, S., and Brickmann, J. *J. Mol. Graphics* 1994, **12,** 98
48 Duncan, B.S. and Olson, A.J. *J. Mol. Graphics* 1995, **13,** 250
49 Laskowski, R.A. *J. Mol. Graphics* 1995, **13,** 323
50 Masuya, M. and Doi, J. *J. Mol. Graphics* 1995, **13,** 331
51 Van Allen, D.R., *MolTube.CPP.* Molecular Modeling Laboratory, Laurentian University, Sudbury, Ontario, Canada, 1996
52 Thomas, D.J. *J. Mol. Graphics* 1994, **12,** 146
53 Lancaster, P. and Salkauskas, K. *Curve and Surface Fitting: An Introduction.* Academic Press, London, 1986
54 Hypercube. *HyperChem 4.0.* Hypercube, Inc., Waterloo, Canada, 1994
55 Sayle, R. *RasWin Molecular Graphics (RasMol2, Windows Version 2.2).* Glaxo Research and Development Greenford, Middlesex, UK, 1993.
56 Arteca, G.A. *Biopolymers* 1993, **33,** 1829
57 Arteca, G.A. *Can. J. Chem.* 1995, **73,** 241
58 Du, Q. and Arteca, G. *J. Comput.-Aided Mol. Design* 1996, **10,** 133
59 Arteca, G., Du, Q., and Payette, M. *Alv.FOR.* Molecular Modeling Laboratory, Laurentian University, Sudbury, Ontario, Canada 1994